Quest Journals
Journal of Research in Environmental and Earth Sciences
Volume 8 ~ Issue 3 (2022) pp: 01-10
ISSN(Online) :2348-2532
www.questjournals.org

Research Paper

Chlorophyll Distribution and Variability at the Surface of the Indian Ocean

Oldemar de Oliveira Carvalho Junior
Instituto Ekko Brasil, Research & Project Office, Santa Catarina Island, Brazil
Corresponding Author: Oldemar de Oliveira Carvalho Junior

***ABSTRACT**: Surface chlorophyll in the oceans can be a valuable tool for tracing surface water mass movement and analysing water mass mixing, important to the formation of water masses within the global oceanic circulation. It is observed differences in chlorophyll concentration in the oceanic surface layer from one oceanic region to the other. This work establishes a distribution and variability of chlorophyll in the surface layer of the tropical Indian Ocean (25°N to 30°S and 30°E to 120°E). It is based on analysis of semi-annual and annual amplitudes of chlorophyll. It is discussed the different physical processes that can be involved with the variability of chlorophyll. This analysis is strongly restricted to the available data sets. The geographical representation of the variability and distribution of the surface chlorophyll agrees well with the theoretical frame of reference.*

***KEYWORDS**: Remote Sensing, Harmonic Analysis, Productivity*

***R**eceived 18 Feb, 2022; **R**evised 01 Mar, 2022; **A**ccepted 03 Mar, 2022 © The author(s) 2022.*
P**ublished with open access at **www.questjournals.org

I. INTRODUCTION

The analysis of surface chlorophyll distribution represents an important data in ocean's primary production. It is a difficult task, as temporal variability at the surface is extreme and data are normally scarce. Techniques to measure primary productivity have been commonly designed to be used by commercial and scientific ships. Despite the importance of data collected by this method, it results in sparse spatial and temporal coverage and requires considerable time to cover large areas. Satellites, on the other hand, are more efficient in producing synoptic and large-scale information such as the study of phytoplankton distribution based on the colour of the ocean, such as the Coastal Zone Colour Scanner Experiment (CZCS) on Nimbus satellites.

Many attempts have been made to measure surface water quality by satellite remote sensing [1] and [2]. Examples of the use of remote sensing to estimate and map water quality variables can be found in the literature using both, airborne [3] and satellite [4]. Parameters usually measured include altimetry, temperature, suspended sediment, turbidity, and chlorophyll-*a*. Studies of phytoplankton in the Indian Ocean, using a satellite, have been conducted by [5] and [6].

The air-sea interface represents a common boundary shared by the ocean and atmosphere. Solar radiation, wind stress, Ekman pumping, heat exchange, among other atmospheric and oceanographic processes, result in large seasonal and inter-annual variability of the water properties at the ocean surface. To clarify the processes currently involved with the surface water properties, it is convenient to treat sea surface chlorophyll (SSC) as pseudo-harmonic terms.

The harmonic terms can be derived from the long-time series of these parameters, from sources such as the NOAA/CZCS Data Set. Therefore, it is possible that an annual cycle of SSC be treated as a simple harmonic term, as it tends to be repeated in a regular cycle. This annual oscillation, however, can be the product of opposing influences, for example the two phases of the monsoons in the Indian Ocean. It is not very common to find harmonic analysis in the oceanographic literature but some authors [7], [8], [9], [10], [11], and [12] have introduced the sub-harmonic six-monthly term to deal with the perturbations observed in the oceanic mixed layer.

When studying such records, the harmonic terms can be stationary, as the averages and corresponding autocorrelations are not expected to vary significantly in a long period of time. In this way, the stationary time series can then be expressed symbolically by Fourier series as a cosine function in which the first and second harmonic terms are multiplied by the maximum amplitude of the variable and added to the mean annual parameter. The modelled data can thus be expressed as:

$$O(t) = \bar{O} + cos(\omega_a \times t - a) + B \times cos(\omega_s \times t - b)$$

where:

$O(t)$ = observed value as a function of time where t is time in days, since the start of an arbitrary year,

$\bar{O}$ = mean value over the period,

A = Amplitude of the annual harmonic component,

B = Amplitude of the semi-annual harmonic component,

a = Phase-lag of the annual component,

b = Phase-lag of the semi-annual component,

ω_a = Angular frequency $2\pi/365.25$ which represents the increment in phase per unit time, t, of the annual harmonic component,

ω_s = ditto for the semi-annual component but $2\pi/182.62$,

ω_a x t - a = phase of the annual harmonic, π

ω_s x t - b = phase of the semi-annual harmonic.

Values of *O, A, B, a and b* are to be determined by analysis. *O* represents the average annual chlorophyll and is a positive constant. The amplitude value (*A or B*) is also a positive constant that represents the amplitude of the motion and so its maximum departure from the mean value as the term oscillates within a range of + or -. Phase-lag is expressed in degrees and increments at 30° per month for the first harmonic and 60° per month for the second, where phase is zero it implies that a maximum occurs in beginning-January. It expresses the average time when the maximum of SSC occurs within the annual cycle. For example, phase of 120° corresponds to first of April, 150° first of May and 270° first of October.

The aim of this work is to establish a convenient tool to experiment and analyse the complexities of the yearly cycles of monthly means from the available data sets for chlorophyll in the surface waters of the Indian Ocean. These monthly mean parameters are subject to a harmonic analysis using the two simple fundamental pseudo-periodic terms of annual and semi-annual period. The idea is first to examine the quality and adequacy of the fit of the two components harmonic to the observed term variability, averaged over a long timescale. Second is to consider the influence and phasing of the terms to help to discuss the physical processes that might be with the variability of the monthly means of SSC.

This approach is not entirely new. In fact, similar analyses have been performed in the past for the north Pacific, English Channel, Irish Sea [7], and for the Indian Ocean [13] and [14]. Annual and semi-annual harmonics have also been applied to the examination of wind, temperature, and currents as a function of depth in the North Pacific Ocean [15] and [16].

The identification of the spatial distributions of amplitude and phase of the two harmonics and their implied interactions, over a super-imposed grid, can be of great advantage for the study of the oceanic mixed layer. A potential exists for a closer focus on the basic causal functions of variance in monthly to yearly time scales of air-sea interactions and water mass formation in the region [17].

II. The CZCS Data Set

Chlorophyll data from the CZCS (Coastal Zone Colour Scanner) are used to analyse chlorophyll distribution and variability at the surface of the Indian Ocean. Chlorophyll data were processed by NASA Goddard Space Flight Centre (GSFC). The contents of the grid data are monthly chlorophyll average, converted to Hierarchical Data Format (HDF). Chlorophyll regional images for the Indian Ocean (volume 4, 1994c) are used. The regional images represent monthly data from 1981 to 1986. Details about the contents of the CD-ROM can be found in [18].

The satellite data set includes data from the satellite Nimbus 7 CZCS. Regional pigment concentration is produced by the CZCS. Phytoplankton pigment concentration series data consist of data from 1978 to 1986. Sea Surface pigment concentration is computed from pixel (digital numbers) values using the formulae:

$$Chl = 10^{(0.012 \times DN - 1.4}$$

The unit is in milligrams per cubic meter for pigment concentration. The binary data are converted to ASCII text matrix using Transform software. The data cover a square region with latitudes ranging from 30.3°N to 59.5°S and longitudes ranging from 32.0°E to 122.0°E. Each data value in the matrix represents a 0.176 degree by 0.176 degree region of the ocean. Therefore, the satellite data set, organized in a 512 x 512 pixel scenes, is rearranged in a 5° x 5° grid that corresponds to a latitude and longitude grid.

III. Sea Surface Chlorophyll Distribution

The 5° x 5° grid average sea surface chlorophyll (SSC) is calculated from the CZCS Data Set. Figure 1 shows the contour plots of the SSC for July, August, and September, during the Southwest Monsoon. The open ocean waters exhibit a very low concentration of chlorophyll, below to 0.2 $mg.m^{-3}$. Exception to these low values is the western Arabian Sea that presents chlorophyll values from 0.7 to 3.2 $mg.m^{-3}$ and from 0.7 to 1.3

mg.m^{-3} in the Bay of Bengal. Very low chlorophyll concentrations, below 0.09 mg.m^{-3} are found in central southern Indian Ocean.

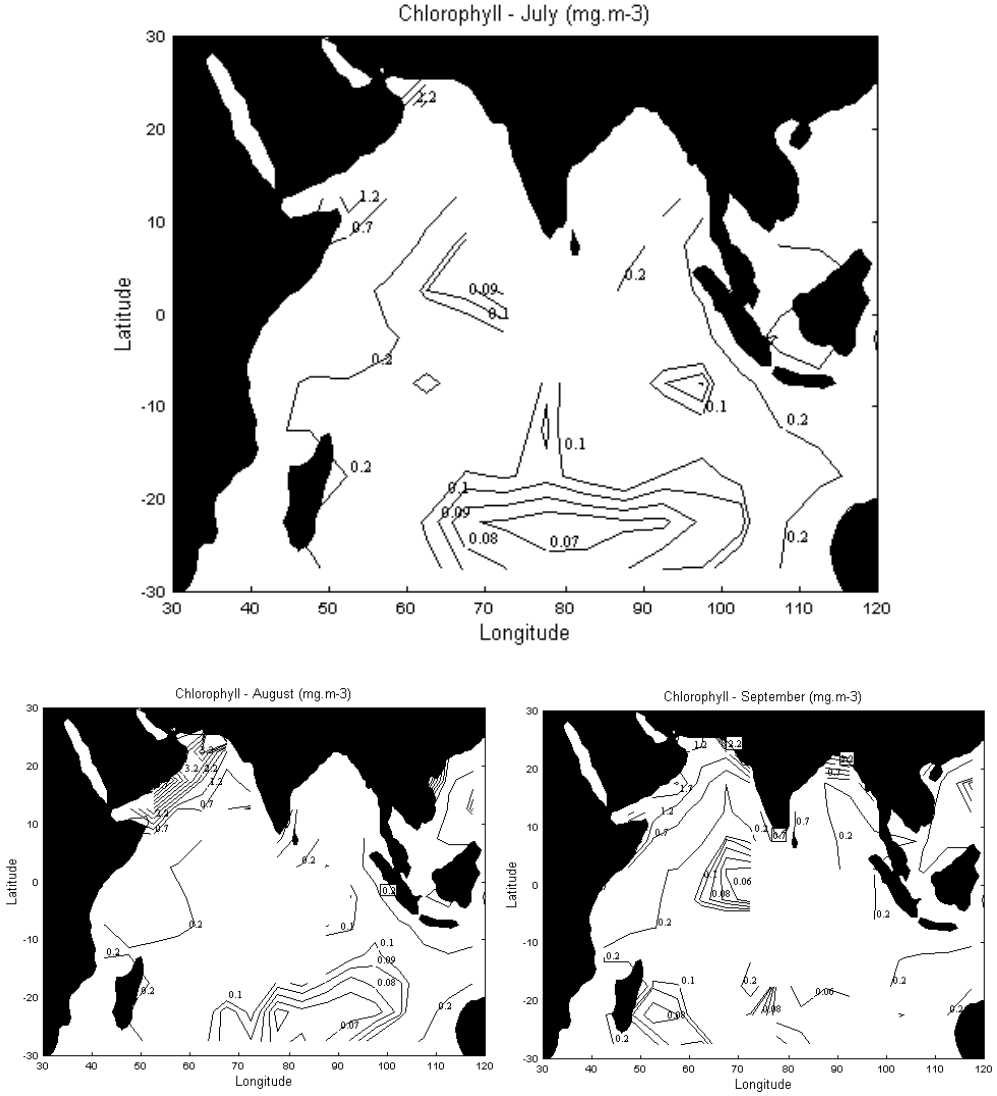

Figure 1: Average Sea surface chlorophyll based on 5 degrees square for the Southwest Monsoon (July, August, and September). Chlorophyll in mg.m^{-3}.

The equatorial region shows low chlorophyll concentration around 0.1 mg.m^{-3}. A zonal chlorophyll contour distribution is observed in the central southern Indian Ocean, while the eastern boundaries exhibit a meridional chlorophyll contour distribution. The highest chlorophyll values (around 3 mg.m^{-3}) are found along the Arabian coast during August.

The 5° x 5° grid average contours of SSC for January, February, and March, during the Northeast Monsoon, can be seen in Figure 2. The contour pattern does not change significantly during the Northeast Monsoon, and most of the southern Indian Ocean shows chlorophyll values below 0.09 mg.m^{-3}. Chlorophyll concentration values are above 0.5 mg.m^{-3} in the north Arabian Sea and North Bay of Bengal. The highest chlorophyll concentration is found at northwest cost of India (3.2 mg.m^{-3}).

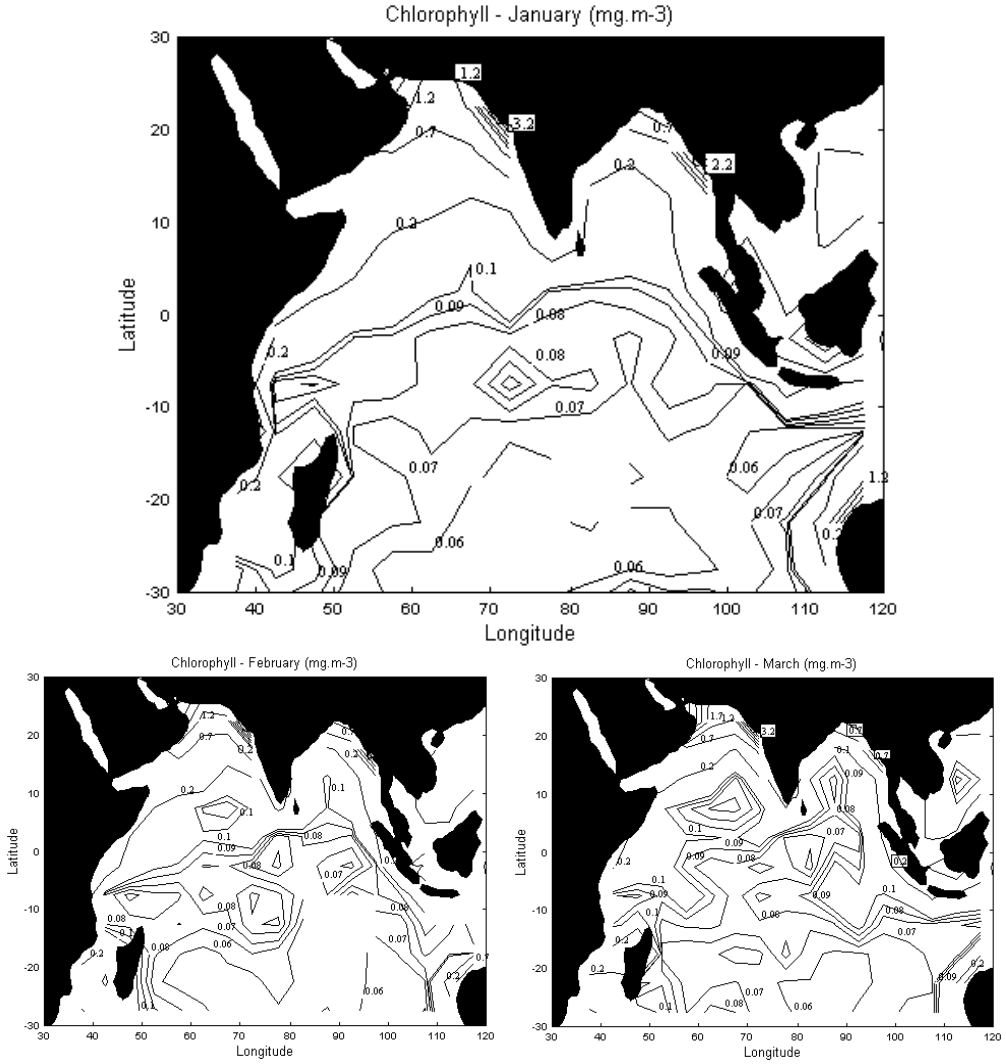

Figure 2: Average SSC based on a 5 degrees square for the Northeast Monsoon (January, February, and March). Chlorophyll in $mg.m^{-3}$.

IV. Annual and Semiannual Cycles of Sea Surface Chlorophyll

The annual variation of chlorophyll amplitudes is shown in Figure 3. The entire southern Indian Ocean shows amplitude values below to 0.05 $mg.m^{-3}$. The amplitudes increase into the Arabian Sea and Bay of Bengal. Maximum values of 1.5 $mg.m^{-3}$ are observed at north of Bay of Bengal and along the Arabian coast.

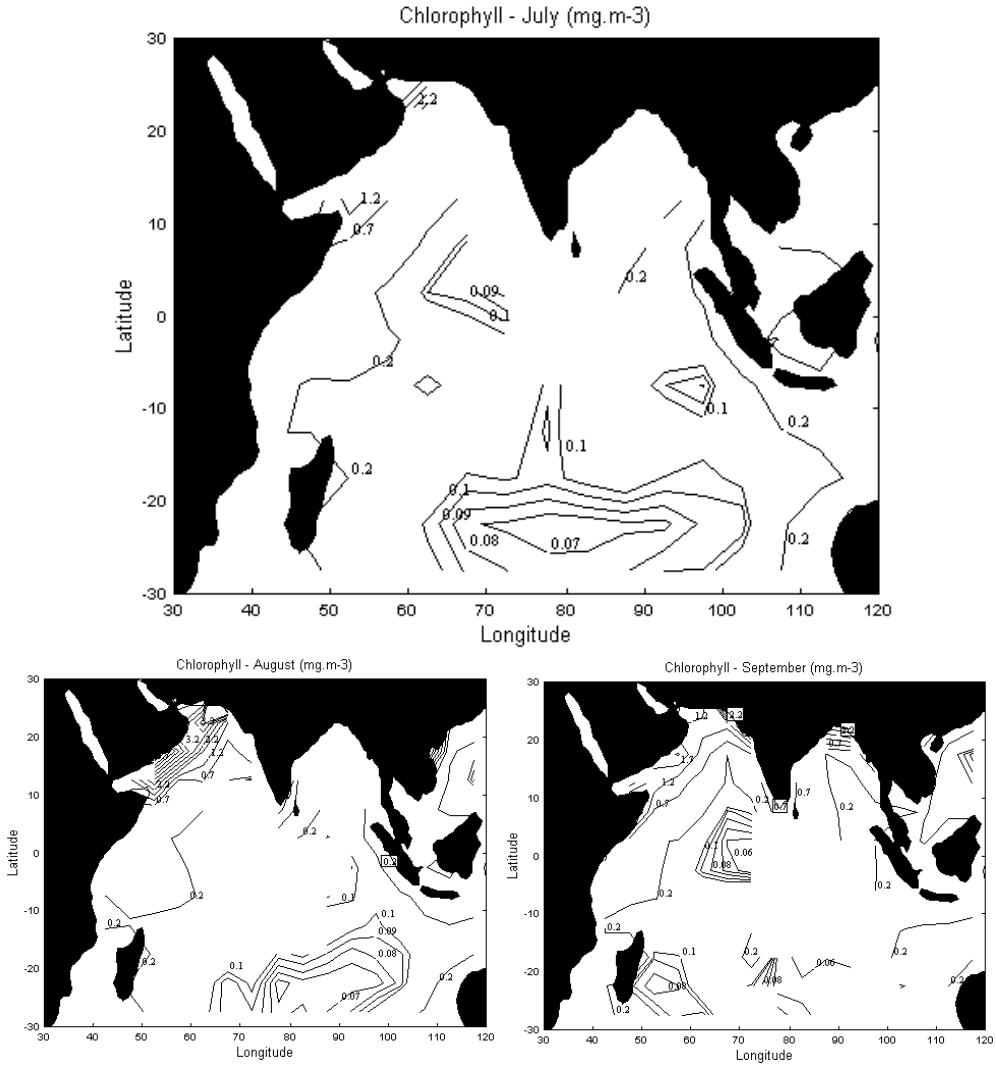

Figure 3: Average Sea surface chlorophyll based on 5 degrees square for the Southwest Monsoon (July, August, and September). Chlorophyll in mg.m^{-3}.

The 5° grid average contours of SSC for January, February, and March, during the Northeast Monsoon, can be seen in Figure 4. The contour pattern does not change significantly during the Northeast Monsoon, and most of the southern Indian Ocean shows chlorophyll values below 0.09 mg.m^{-3}. Chlorophyll concentration values are above 0.5 mg.m-3 in the north Arabian Sea and North Bay of Bengal. The highest chlorophyll concentration is found at northwest cost of India (3.2 mg.m^{-3}).

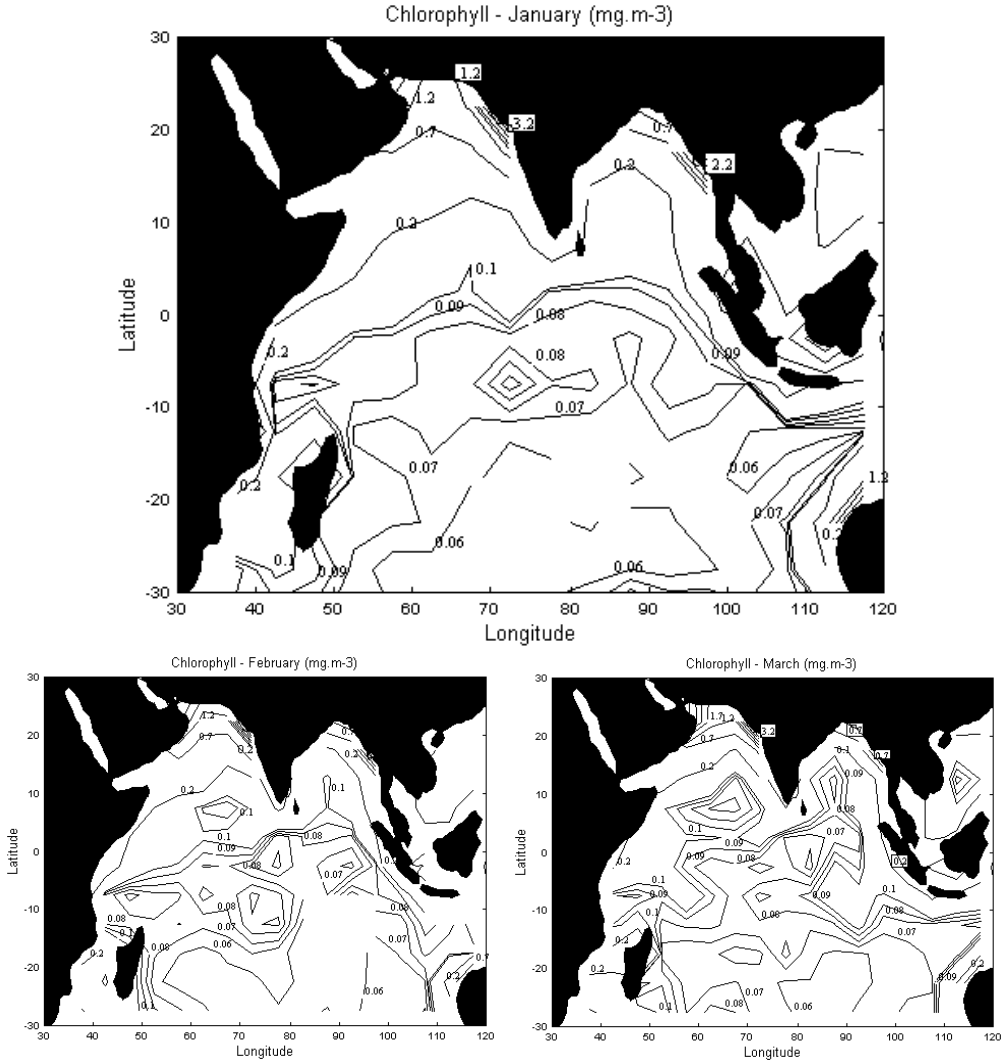

Figure 4: Average SSC based on a 5 degrees square for the Northeast Monsoon (January, February, and March). Chlorophyll in mg.m^{-3}.

V. Sea Surface Chlorophyll - Harmonic Analysis

The distribution of chlorophyll, computed for an average year over a 5 degrees grid, as expressed through the annual and semi-annual harmonic, is shown in Figure 5. The region south of the equator shows amplitude values of the annual and semi-annual components below 0.05 mg.m^{-3}. The amplitudes increase into the Arabian Sea and Bay of Bengal. Maximum values of 1.5 mg.m^{-3} are observed in the northern Indian Ocean, where large inflows of freshwater from river runoff in the Bay of Bengal and the upwellings along the Somali and Arabian coasts are likely to exert some influence on the chlorophyll variability (Figure 5a).

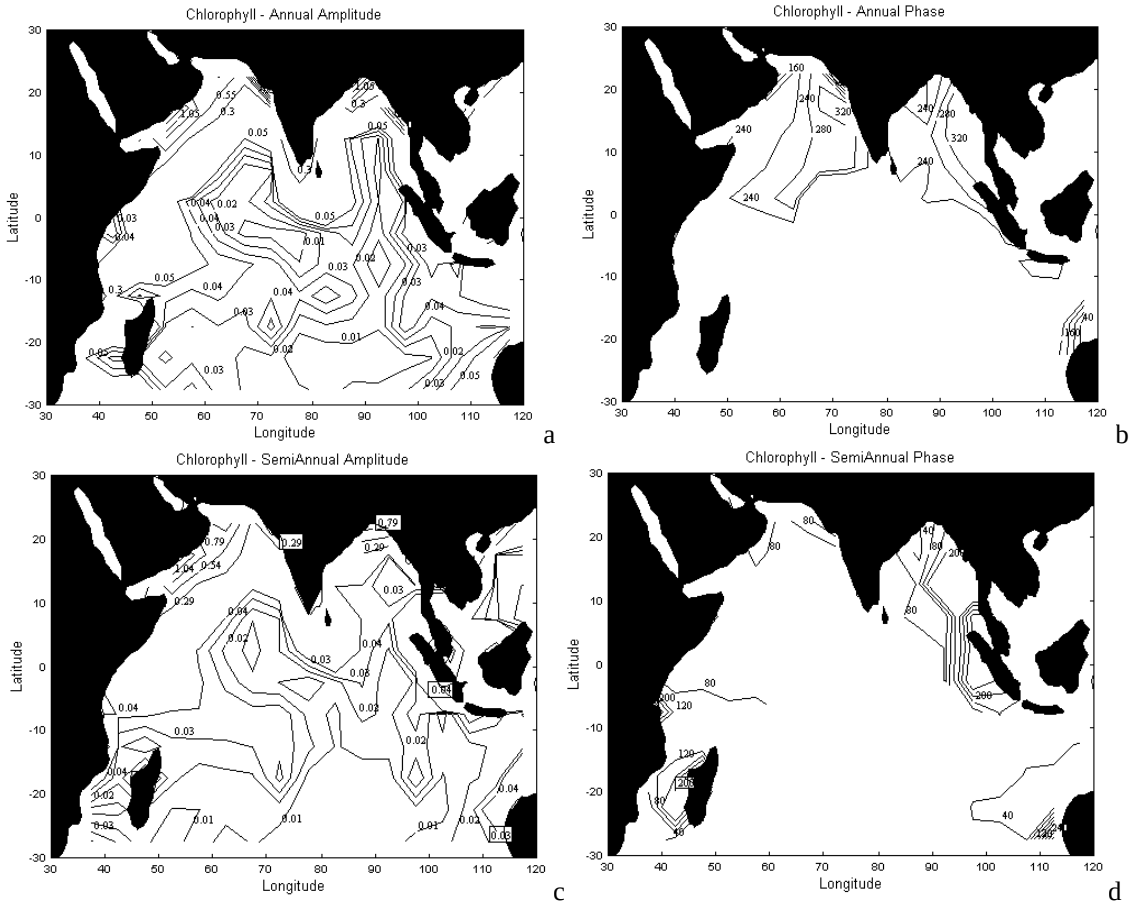

Figure 5: (a). The distribution of chlorophyll (mg.m^{-3}) amplitude for the first harmonic. (b) The distribution of phase-lag of chlorophyll for the first harmonic. (c) The distribution of chlorophyll (mg.m^{-3}) amplitude for the second harmonic. (d) The distribution of phase-lag of chlorophyll for the second harmonic. Phase is ignored where amplitudes are smaller than 0.05 mg.m^{-3}. Amplitude and phase of SSC are calculated from the CZCS data set.

Phase-lag distribution can be observed in Figures 5b (annual) and 5d (semi-annual). Phase lag is shown only where the amplitudes are larger than 0.05 mg.m^{-3}. Maximum for the annual component occurs in late November, along the western Arabian Sea and western Bay of Bengal (Figure 5b). Along the western Indian Ocean, close to the equator, the annual component is maximum at the end of August. This maximum occurs earlier towards the north, in which the maximum at the northernmost part of the Arabian Sea occurs in early June.

In both areas, Arabian Sea and Bay of Bengal, the maximum of the annual component occurs gradually later from west to east. In the southern Indian Ocean, most of the maximum of the annual component occurs between late July and late August. A gradient shift is observed in the equator, around 70°E, which indicates the transition between the southern and Northern Hemisphere.

The distribution of the semi-annual chlorophyll amplitude (Figure 5c) shows larger values in the western Arabian Sea and in the northern part of the Bay of Bengal. Maximum semi-annual amplitudes are found along the Arabian coast, where values are above 1.0 mg.m^{-3}. In the Bay of Bengal, maximum amplitudes are close to 0.8 mg.m^{-3}.

The maximum of the semi-annual component in the north Arabian Sea is during early February and early August (Figure 5d). In the Bay of Bengal, this maximum occurs from late January and late July in the west to early April and early October in the east. In the Arabian Sea, the maximum of the semi-annual component occurs during the peaks of the NE and SW Monsoons.

As an example, Figure 6a shows the degree of fit to the observed record achieved by the two harmonic components and Figure 6b exhibits the two individual harmonic components themselves and their interaction through the year along the Arabian coast. The annual component is seen to have a maximum in August and a minimum during February, which shows a connection with the peaks of the SW Monsoon and NE Monsoon. However, the maximum peak during August must be analysed with care, as it is associated with a large residual error (Figure 6c).

Compared with the annual component, the amplitude of the semi-annual component is slightly smaller in magnitude, with two maxima in February and August and two minima in May and November. The two maxima can also be associated with the two monsoon peaks (February for the NE Monsoon and August for the SW Monsoon) but the two minima seem to be related with the transition months of the monsoons (May and November).

The two harmonic components act in conjunction but struggle to produce the maximum chlorophyll peak during August. This chlorophyll peak is likely to be a result of upwelling and mixing, which are common during this time of the year for this region. The maximum of the annual component can be due to monsoon wind-driven advection which results in a strong northward flow (Somali and East Arabian Current) and light availability, because of larger input of solar radiation during the northern summer.

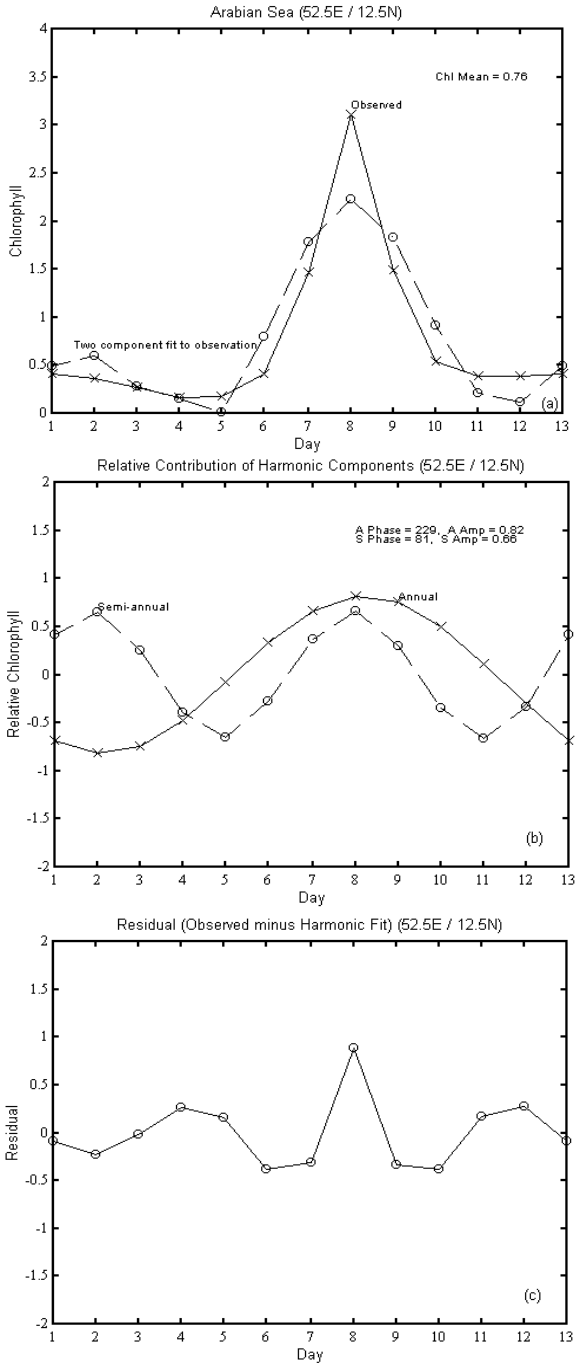

Figure 6: (a) Observed and two components fit to observation ($mg.m^{-3}$). (b) First and second components of the harmonic analysis. (c) Residual plot between observed and harmonic chlorophyll ($mg.m^{-3}$). Time (months) in which 13 is equal to 1 and corresponds to mid-January.

A secondary high of chlorophyll in February is not clear. In fact, it represents a secondary maximum when the chlorophyll concentration is close to 0.5 $mg.m^{-3}$. However, this semi-annual component does little for the combined fit, and it can be taken as a non-existent peak, but a function of inadequate fitting resulted from just two components. During August, the chlorophyll concentration reaches values above 2 $mg.m^{-3}$, which could be associated with the upwelling that occurs during the same period along the Arabian coast. The chlorophyll response to changes in the environment is a highly non-linear manner, which produces a strong, steep increase and decay. This results in an artificial harmonic fit to the data, in which semi-annual and annual components must be interpreted with care.

As can be seen from Figure 6c, large residual errors ranging between -0.08 $mg.m^{-3}$ (January) to 0.88 $mg.m^{-3}$ (August) are observed. These large residuals suggest that the two harmonic components fit has to be accepted with some reservation, since the application of only the two harmonic components seems not to fully explain the chlorophyll variability in this area.

A difference in phase-lag from west to east is observed in the Bay of Bengal. The western part exhibits a maximum of the semi-annual component in early February and early August, while in the eastern part this maximum occurs in early April and early October. Minimum wind stress during April and October, plus maximum river runoff due to high precipitation during the SW Monsoon, could be associated with these maxima in chlorophyll concentration. On the one hand, in the eastern part of the Bay of Bengal the wet season finishes by October and the input of nutrients due to river runoff is likely to remain in the area because of the weak light winds during April and October. On the other hand, the chlorophyll peak during February can be a result of strong wind mixing and the peak during August a combination of a positive net-down-freshwater-flow (ndff) and wind mixing.

VI. Conclusions

The distributions of observed and harmonic SSC reveal the areas of large annual and semi-annual variability in the Indian Ocean surface. Maximum amplitudes of the annual and semi-annual amplitudes of chlorophyll were found along the western Arabian Sea and in the north of the Bay of Bengal.

Overall, the annual component is related to large-scale features of the seasonal solar radiation input and the seasonal monsoons. Basic features associated with the monsoons, such as wind-driven advection, can be representing significant influence on the annual term. The semi-annual component is related to local and regional influences, which are superimposed upon the basic pattern defined by the annual term. These local and regional influences are the results of different processes such as upwelling and non-directional effect of wind stress (e.g. evaporation, precipitation and mixing).

This work showed that the resulted fitting for chlorophyll from just two harmonic components results in some large residual errors. Therefore, the results suggest that the two-component fit has to be accepted with some reservation to fully explain the chlorophyll variability.

Although harmonic analysis can be applied to the study of chlorophyll variability, it does not provide a quantification of the variables involved in this variability. The harmonic components can be associated with the possible physical processes related to this variability, but they cannot be properly quantified.

To identify and quantify the variables related to these areas of large annual and semi-annual variability, a multiple regression analysis could be applied, and it is suggested for future research on this subject. Combination of physical and biological processes which can affect SSC in the Indian Ocean includes the analysis of the components of pseudostress wind, Ekman pumping, wind magnitude and ndff. This approach, together with a simple theoretical frame of reference, can result in a good attempt to explain and quantify the observed annual and semi-annual variability.

REFERENCES

[1]. Ritchie, J. C., & Cooper, C. M. (1987). Comparison of Landsat MSS Pixel Array Sizes for Estimating Water Quality. *PHOTOGRAMMETRIC ENGINEERING AND REMOTE SENSING*, *53*(11), 1549–1553. https://www.asprs.org/wp-content/uploads/pers/1987journal/nov/1987_nov_1549-1553.pdf

[2]. Markogianni, V., Kalivas, D., Petropoulos, G. P., & Dimitriou, E. (2018). An Appraisal of the Potential of Landsat 8 in Estimating Chlorophyll-a, Ammonium Concentrations and Other Water Quality Indicators. *Remote Sensing*, *10*(7), 1018. https://doi.org/10.3390/rs10071018

[3]. Garcia, C. A. E., & Robinson, I. S. (1991). Chlorophyll-a mapping using Airborne Thematic Mapper in the Bristol Channel (South Gower Coastline). *International Journal of Remote Sensing*, *12*(10), 2073–2086. https://doi.org/10.1080/01431169108955237

[4]. Saberioon, M., Brom, J., Nedbal, V., Souček, P., & Císař, P. (2020). Chlorophyll-a and total suspended solids retrieval and mapping using Sentinel-2A and machine learning for inland waters. *Ecological Indicators*, *113*, 106236. https://doi.org/10.1016/j.ecolind.2020.106236

[5]. Demarcq, H., Noyon, M., & Roberts, M. J. (2020). Satellite observations of phytoplankton enrichments around seamounts in the South West Indian Ocean with a special focus on the Walters Shoal. *Deep Sea Research Part II: Topical Studies in Oceanography*, *176*, 104800. https://doi.org/10.1016/j.dsr2.2020.104800

[6]. Barik, K. K., Baliarsingh, S. K., Jena, A. K., Srichandan, S., Samanta, A., & Lotliker, A. A. (2020). Satellite Retrieved Spatio-temporal Variability of Phytoplankton Size Classes in the Arabian Sea. *Journal of the Indian Society of Remote Sensing*, *48*(10), 1413–1419. https://doi.org/10.1007/s12524-020-01165-w

[7]. Wyrtki, K. (1965). The Annual and Semiannual Variation of Sea Surface Temperature in the North Pacific Ocean1. *Limnology and Oceanography*, *10*(3), 307–313. https://doi.org/10.4319/lo.1965.10.3.0307
[8]. White, W. B. (1978). A Wind-Driven Model Experiment of the Seasonal Cycle of the Main Thermocline in the Interior Midlatitude North Pacific. *Journal of Physical Oceanography*, *8*(5), 818–824. https://doi.org/10.1175/1520-0485(1978)008<0818:AWDMEO>2.0.CO;2
[9]. Levitus, S. (1987). A Comparison of the Annual Cycle of Two Sea Surface Temperature Climatologies of the World Ocean. *Journal of Physical Oceanography*, *17*(2), 197–214. https://doi.org/10.1175/1520-0485(1987)017<0197:ACOTAC>2.0.CO;2
[10]. Herrera-Cervantes, H., & Herrera-Cervantes, H. (2019). Sea surface temperature, ocean color and wind forcing patterns in the Bay of La Paz, Gulf of California: Seasonal variability. *Atmósfera*, *32*(1), 25–38. https://doi.org/10.20937/atm.2019.32.01.03
[11]. Susanto, R. D., Pan, J., & Devlin, A. T. (2019). Tidal Mixing Signatures in the Hong Kong Coastal Waters from Satellite-Derived Sea Surface Temperature. *Remote Sensing*, *11*(1), 5. https://doi.org/10.3390/rs11010005
[12]. Habibullah, A. D., & Tarya, A. (2021). Sea surface temperature variability in Indonesia and its relation to regional climate indices. *IOP Conference Series: Earth and Environmental Science*, *925*(1), 012008. https://doi.org/10.1088/1755-1315/925/1/012008
[13]. Unnikrishnan, A. S., Prasanna Kumar, S., & Navelkar, G. S. (1997). Large-scale processes in the upper layers of the Indian Ocean inferred from temperature climatology. *Journal of Marine Research*, *55*(1), 93–115. https://doi.org/10.1357/0022240973224490
[14]. McPhaden, M. J. (1982). Variability in the central equatorial Indian Ocean. I. Ocean dynamics. *Journal of Marine Research*, *40*(1), 157–176. https://scholar.google.com/scholar_lookup?title=Variability+in+the+central+equatorial+Indian+Ocean.+I.+Ocean+dynamics.&author=McPhaden+M.J.&publication_year=1982
[15]. Bograd, S., Schwing, F., Mendelssohn, R., & Green-Jessen, P. (2002). On the changing seasonality over the North Pacific. *Geophysical Research Letters*, *29*(9), 47-1-47–4. https://doi.org/10.1029/2001GL013790
[16]. Giglio, D., Gille, S. T., Cornuelle, B. D., Subramanian, A. C., Turk, F. J., Hristova-Veleva, S., & Northcott, D. (2022). Annual Modulation of Diurnal Winds in the Tropical Oceans. *Remote Sensing*, *14*(3), 459. https://doi.org/10.3390/rs14030459
[17]. Carvalho Junior, O. de O. (2015). Massas de água na superfície dos oceanos e circulação oceânica (1st ed.). Novas Edicoes Academicas.
[18]. Mass, C. F. (1993). The Application of Compact Discs (CD-ROM) in the Atmospheric Sciences and Related Fields: An Update. *Bulletin of the American Meteorological Society*, *74*(10), 1901–1908. https://www.jstor.org/stable/26230679